

Mesons and tachyons with confinement and chiral restoration

P. Bicudo

Dep. Física and CFTP, Instituto Superior Técnico, Av. Rovisco Pais, 1049-001 Lisboa, Portugal

(Received 18 June 2006; published 1 September 2006)

In this paper the spectrum of quark-antiquark systems, including light mesons and tachyons, is studied in the true vacuum and in the chiral invariant vacuum. The mass gap equation for the vacua and the Salpeter-RPA equation for the mesons are solved for a simple chiral invariant and confining quark model. At $T = 0$ and in the true vacuum, the scalar and pseudoscalar, or the vector and axial vector are not degenerate, and in the chiral limit, the pseudoscalar groundstates are Goldstone bosons. At $T = 0$ the chiral invariant vacuum is an unstable vacuum, decaying through an infinite number of scalar and pseudoscalar tachyons. Nevertheless the axialvector and vector remain mesons, with real masses. To illustrate the chiral restoration, an arbitrary path between the two vacua is also studied. Different families of light-light and heavy-light mesons, sensitive to chiral restoration, are also studied. At higher temperatures the potential must be suppressed, and the chiral symmetry can be restored without tachyons, but then all mesons have small real masses. Implications for heavy-ion collisions, in particular, for the recent vector meson spectra measured by the NA60 collaboration, are discussed.

DOI: [10.1103/PhysRevD.74.065001](https://doi.org/10.1103/PhysRevD.74.065001)

PACS numbers: 11.30.Rd, 12.38.-t, 12.38.Mh, 12.39.Ki

I. INTRODUCTION

Very recently, the precise di-muon measurement in heavy-ion indium-indium collisions by NA60 [1–5] collaboration provided an exceptional probe to observe vector mesons in excited vacua. The masses of vector mesons in excited vacua, have been extensively modeled, with different results, since Brown and Rho [6–9] proposed the scaling of the light-light vector mesons with the restoration of chiral symmetry. Notice that tachyons may also occur. When there are only mesons in the vacuum, the vacuum is a minimum. It is then stable when the minimum is absolute, or metastable when the minimum is local because then the vacuum can decay through tunnelling. However when both mesons and tachyons occur, the vacuum is a saddle point. The tachyons indicate the decay directions of the vacuum, and thus the vacuum is unstable, it is a false vacuum.

Here I compare the mesons and tachyons in the false chiral invariant vacuum and in the true vacuum, in the framework of a chiral invariant and confining potential. Notice that, in the true vacuum of QCD, quarks are confined. On the other hand, in the excited vacuum, chiral restoration is expected. Therefore a framework with a confining and chiral invariant quark interaction is convenient to study mesons and tachyons in the two vacua. The present study, with confinement, upgrades our knowledge of vacua and of vacuum fluctuations in hadronic models.

Similar studies, before this one, have only been performed in nonconfining models. For instance vacua properties of the nonconfining sigma model [10–12] and Nambu and Jona-Lasinio model [13] have been explored in detail [14], including surprising unstabilities led by the 't Hooft $U_A(1)$ breaking determinant [15]. In the simplest scenarios, the vacua manifold of these models has the well known Mexican hat shape, where the chiral invariant unstable vacuum has a finite number of tachyons. The tachy-

ons in the flavour SU(2) sigma model occur in the scalar σ and in the pseudoscalar π^+ , π^0 , π^- channels. So in the sigma model there are four tachyons in the false chiral invariant vacuum, while in the true chiral symmetry breaking vacuum there is one massive meson, the scalar σ and three pseudoscalar mesons π^+ , π^0 , π^- . In the chiral limit the pseudoscalar mesons are goldstone bosons, in the borderline between mesons and tachyons.

However, when quarks suffer a confining potential, the tachyon structure of the false chiral invariant vacuum possibly differs from the one of the sigma model or the one of the Nambu and Jona-Lasinio model. In the true vacuum, the confining quark models have an infinite number of states in each channel, while the sigma model of the Nambu and Jona-Lasinio model only have a finite number of mesons. Other differences also occur. Le Yaouanc *et al.* [16] found that, even at high temperatures, the confining potential prevents a phase transition from the chiral symmetry breaking vacuum to the chiral invariant vacuum. Le Yaouanc, Oliver, Ono, Pène and Raynal, [17] also found that, with a harmonic confinement, there is an infinite tower of excited vacua, interpolating between the true chiral symmetry breaking vacuum to the highest chiral invariant vacuum. This result was recently generalized to any confining potential by PB and Nefediev [18]. The existence of tachyons in the chiral invariant vacuum of a confining quark model was already signalled by Le Yaouanc, Oliver, Ono, Pène and Raynal, [17]. Here these tachyons are studied in detail.

Because the present problem is quite technical, and because it is not clear yet what is the best chiral invariant and confining quark model, for clarity I now use the framework of the simplest confining and chiral invariant quark model [17,19,20].

Notice that a calibration problem exists in chiral computations. The full hadron spectrum remains to be correctly

reproduced. When the quarks were discovered, it was realized that the main difficulty of the quark model consisted in understanding the low pion mass. But Nambu and Jona-Lasinio [13] had already shown that the spontaneous dynamical breaking of global chiral symmetry provides a mechanism for the generation of the constituent fermion mass and for the almost vanishing mass of the pion. This mechanism was extended to the quark model by le Yaouanc, Oliver, Ono, Pène and Raynal with the Salpeter equations in Dirac structure [17] and by PB and Ribeiro with the equivalent Salpeter equations in a form [19] identical to the Random Phase Approximation (RPA) equations of Llanes-Estrada and Cotanch [21]. These chiral quark models also comply with the PCAC theorems, say the Gell-Mann Oakes and Renner relation [17,20], the Adler Zero [22–24], the Goldberger-Treiman Relation [22,25], or the Weinberg Theorem [22,23,26]. Possibly a chiral quark model with the correct spin-tensor potentials will eventually reproduce the full spectrum of hadrons [19]. Nevertheless this is only a quantitative problem, qualitatively the simple model used here is sufficient to study several implications of chiral symmetry and confinement.

Recently, the full mesonic spin-tensor potentials of the present simple model were determined for a quark and an antiquark with different isospin [27]. Here I exactly solve these boundstate equations of mesons and tachyons in different vacua. Importantly, the hamiltonian of this model can be approximately derived from QCD,

$$\begin{aligned}
H = & \int d^3x \left[\psi^\dagger(x) (m_0 \beta - i \vec{\alpha} \cdot \vec{\nabla}) \psi(x) \right. \\
& + \frac{1}{2} g^2 \int d^4y \bar{\psi}(x) \gamma^\mu \frac{\lambda^a}{2} \psi(x) \\
& \times \langle A_\mu^a(x) A_\nu^b(y) \rangle \bar{\psi}(y) \gamma^\nu \frac{\lambda^b}{2} \psi(y) + \dots \quad (1)
\end{aligned}$$

up to the first cumulant order, of two gluons [28–31], which can be evaluated in the modified coordinate gauge,

$$g^2 \langle A_\mu^a(x) A_\nu^b(y) \rangle \simeq -\frac{3}{4} \delta_{ab} g_{\mu 0} g_{\nu 0} [K_0^3 (\mathbf{x} - \mathbf{y})^2 - U] \quad (2)$$

and this is a simple density-density harmonic effective confining interaction. m_0 is the current mass of the quark. The infrared constant U confines the quarks but the meson spectrum is completely insensitive to it. The important parameter is the potential strength K_0 , the only physical scale in the interaction. In the true chiral symmetry breaking vacuum $K_0 \simeq 0.3 \pm 0.05$ GeV fits reasonably the hadron spectra. However in the chiral invariant vacuum the potential strength K_0 is supposed to be greatly suppressed. For simplicity, I will consider a vanishing light quark m_0 and all physical results will scale only with the potential strength K_0 .

I now address the meson and tachyon spectrum in different vacua. In Sec. II the quark mass gap equation and the

bound state quark-antiquark equation are reviewed. In Sec. III the mass gap and boundstate equations are solved numerically and the spectrum is studied in an arbitrary interpolation between the true and the chiral invariant vacuum. In Sec. IV the tachyons solutions of the bound-state equation are analytically studied. These first studies are performed at vanishing temperature. However in heavy-ion collisions finite temperatures are reached, sufficient for a QCD phase transition. The conclusion is presented in Sec. V, including the estimation of temperature effects on the spectra.

II. $T = 0$ MASS GAP AND BOUNDSTATE EQUATIONS

The relativistic invariant Dirac-Feynman propagators [17], can be decomposed in the quark and antiquark Bethe-Goldstone propagators [20], close to the formalism of nonrelativistic quark models,

$$\begin{aligned}
S_{\text{Dirac}}(k_0, \vec{k}) &= \frac{i}{\not{k} - m + i\epsilon} \\
&= \frac{i}{k_0 - E(k) + i\epsilon} \sum_s u_s u_s^\dagger \beta \\
&\quad - \frac{i}{-k_0 - E(k) + i\epsilon} \sum_s v_s v_s^\dagger \beta, \\
u_s(\mathbf{k}) &= \left[\sqrt{\frac{1+S}{2}} + \sqrt{\frac{1-S}{2}} \hat{k} \cdot \vec{\sigma} \gamma_5 \right] u_s(0), \\
v_s(\mathbf{k}) &= \left[\sqrt{\frac{1+S}{2}} - \sqrt{\frac{1-S}{2}} \hat{k} \cdot \vec{\sigma} \gamma_5 \right] v_s(0), \\
&= -i \sigma_2 \gamma_5 u_s^*(\mathbf{k}), \quad (3)
\end{aligned}$$

where $S = \sin(\varphi) = \frac{m_c}{\sqrt{k^2 + m_c^2}}$, $C = \cos(\varphi) = \frac{k}{\sqrt{k^2 + m_c^2}}$ and φ is a chiral angle. In the non condensed vacuum, φ is equal to $\arctan \frac{m_0}{k}$, but φ is not determined from the onset when chiral symmetry breaking occurs. In the physical vacuum, the constituent quark mass $m_c(k)$, or the chiral angle $\varphi(k) = \arctan \frac{m_c(k)}{k}$, is a variational function which is determined by the mass gap equation. Examples of solutions, for different light current quark masses m_0 , are depicted in Fig. 1. For simplicity in the remaining of this paper $m_0 = 0$ will be assumed, nevertheless the effect of a finite current quark mass can be estimated with a small increase of the dynamically generated constituent quark mass m_c .

Then there are three equivalent methods to find the true and stable vacuum, where constituent quarks acquire the constituent mass. One method consists in assuming a quark-antiquark 3P_0 condensed vacuum, and in minimizing the vacuum energy density. A second method consists in rotating the quark and antiquark fields with a Bogoliubov-Valatin canonical transformation to diagonalize the terms in the hamiltonian with two quark or antiquark second quantized fields. A third method consists in

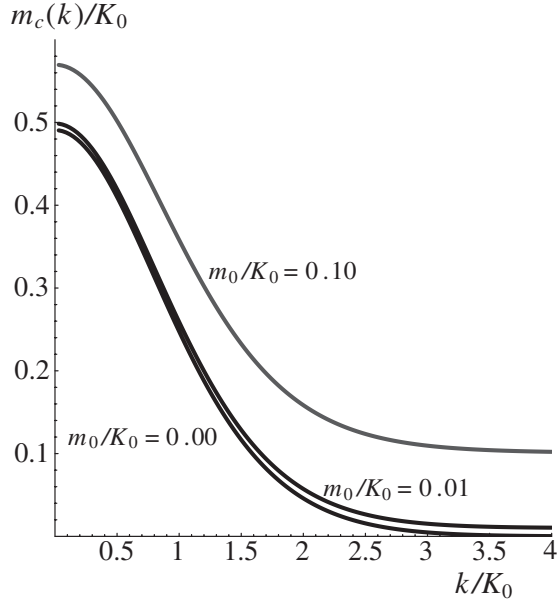


FIG. 1. The constituent quark masses $m_c(k)$, solutions of the mass gap equation, for different current quark masses m_0 .

solving the Schwinger-Dyson equations for the propagators. Any of these methods lead to the same mass gap equation and to the quark dispersion relation. Here I replace the propagator of Eq. (3) in the Schwinger-Dyson equation,

$$\begin{aligned}
 0 &= u_s^\dagger(k) \left\{ k\hat{k} \cdot \vec{\alpha} + m_0\beta - \int \frac{dw'}{2\pi} \frac{d^3k'}{(2\pi)^3} iV(k-k') \right. \\
 &\quad \left. \times \sum_{s'} \left[\frac{u(k')_{s'} u^\dagger(k')_{s'}}{w' - E(k') + i\epsilon} - \frac{v(k')_{s'} v^\dagger(k')_{s'}}{-w' - E(k') + i\epsilon} \right] \right\} v_{s''}(k) \\
 E(k) &= u_s^\dagger(k) \left\{ k\hat{k} \cdot \vec{\alpha} + m_0\beta - \int \frac{dw'}{2\pi} \frac{d^3k'}{(2\pi)^3} iV(k-k') \right. \\
 &\quad \left. \times \sum_{s'} \left[\frac{u(k')_{s'} u^\dagger(k')_{s'}}{w' - E(k') + i\epsilon} - \frac{v(k')_{s'} v^\dagger(k')_{s'}}{-w' - E(k') + i\epsilon} \right] \right\} u_s(k),
 \end{aligned} \tag{4}$$

where, with the simple density-density harmonic interaction [17], the integral of the potential is a laplacian and the mass gap equation and the quark energy are finally,

$$\begin{aligned}
 \Delta\varphi(k) &= 2kS(k) - 2m_0C(k) - \frac{2S(k)C(k)}{k^2} \\
 E(k) &= kC(k) + m_0S(k) - \frac{\varphi'(k)^2}{2} - \frac{C(k)^2}{k^2} + \frac{U}{2}.
 \end{aligned} \tag{5}$$

Numerically, this equation is a nonlinear ordinary differential equation. It can be solved with the Runge-Kutta and shooting method. Examples of solutions for the current quark mass $m_c(k) = k \tan\varphi$, for different current quark masses m_0 , are depicted in Fig. 1.

The Salpeter-RPA equations for a meson (a color singlet quark-antiquark bound state) can be derived from the Lippman-Schwinger equations for a quark and an antiquark, or replacing the propagator of Eq. (3) in the Bethe-Salpeter equation. In either way, one gets [20]

$$\begin{aligned}
 \phi^+(k, P) &= \frac{u^\dagger(k_1)\chi(k, P)v(k_2)}{+M(P) - E(k_1) - E(k_2)} \\
 \phi^-(k, P) &= \frac{v^\dagger(k_1)\chi(k, P)u(k_2)}{-M(P) - E(k_1) - E(k_2)} \\
 \chi(k, P) &= \int \frac{d^3k'}{(2\pi)^3} V(k-k') [u(k'_1)\phi^+(k', P)v^\dagger(k'_2) \\
 &\quad + v(k'_1)\phi^-(k', P)u^\dagger(k'_2)]
 \end{aligned} \tag{6}$$

where $k_1 = k + \frac{P}{2}$, $k_2 = k - \frac{P}{2}$ and P is the total momentum of the meson. Notice that, solving for χ , one gets the Salpeter equations of Le Yaouanc *et al.* [17].

The Salpeter-RPA equations of PB *et al.* [19] and of Llanes-Estrada *et al.* [21] are obtained deriving the equation for the positive energy wave function ϕ^+ and for the negative energy wave function ϕ^- . The relativistic equal time equations have the double of coupled equations than the Schrödinger equation, although in many cases the negative energy components can be quite small. This re-

TABLE I. Matrix elements of the spin-dependent potentials.

$2S+1L_J$	$\delta_{S_q, S_{\bar{q}}}$	$\mathbf{S}_q \cdot \mathbf{S}_{\bar{q}}$	$(\mathbf{S}_q + \mathbf{S}_{\bar{q}}) \cdot \mathbf{L}$	$(\mathbf{S}_q - \mathbf{S}_{\bar{q}}) \cdot \mathbf{L}$	tensor
1S_0	1	-3/4	0	0	0
3P_0	1	1/4	-2	0	-1/3
3S_1	1	1/4	0	0	0
3D_1	1	1/4	-3	0	-1/6
$^3S_1 \leftrightarrow ^3D_1$	0	0	0	0	$\sqrt{2}/6$
1P_1	1	-3/4	0	0	0
3P_1	1	1/4	-1	0	1/6
$^1P_1 \leftrightarrow ^3P_1$	0	0	0	$\sqrt{2}$	0

TABLE II. The positive and negative energy spin-independent, spin-spin, spin-orbit and tensor potentials are shown, for the simple density-density harmonic model of Eq. (2). $\varphi'(k)$, $C(k)$ and $\mathcal{G}(k) = 1 - S(k)$ are all functions of the constituent quark (antiquark) mass.

	$V^{++} = V^{--}$
spin-indep.	$-\frac{d^2}{dk^2} + \frac{1}{k^2} + \frac{1}{4}(\varphi_q'^2 + \varphi_{\bar{q}}'^2) + \frac{1}{k^2}(\mathcal{G}_q + \mathcal{G}_{\bar{q}}) - U$
spin-spin	$\frac{4}{3k^2} \mathcal{G}_q \mathcal{G}_{\bar{q}} \mathbf{S}_q \cdot \mathbf{S}_{\bar{q}}$
spin-orbit	$\frac{1}{k^2} [(\mathcal{G}_q + \mathcal{G}_{\bar{q}})(\mathbf{S}_q + \mathbf{S}_{\bar{q}}) + (\mathcal{G}_q - \mathcal{G}_{\bar{q}})(\mathbf{S}_q - \mathbf{S}_{\bar{q}})] \cdot \mathbf{L}$
tensor	$-\frac{2}{k^2} \mathcal{G}_q \mathcal{G}_{\bar{q}} [(\mathbf{S}_q \cdot \hat{k})(\mathbf{S}_{\bar{q}} \cdot \hat{k}) - \frac{1}{3} \mathbf{S}_q \cdot \mathbf{S}_{\bar{q}}]$
	$V^{+-} = V^{-+}$
spin-indep.	0
spin-spin	$-\frac{4}{3} [\frac{1}{2} \varphi_q' \varphi_{\bar{q}}' + \frac{1}{k^2} C_q C_{\bar{q}}] \mathbf{S}_q \cdot \mathbf{S}_{\bar{q}}$
spin-orbit	0
tensor	$[-2\varphi_q' \varphi_{\bar{q}}' + \frac{2}{k^2} C_q C_{\bar{q}}] [(\mathbf{S}_q \cdot \hat{k})(\mathbf{S}_{\bar{q}} \cdot \hat{k}) - \frac{1}{3} \mathbf{S}_q \cdot \mathbf{S}_{\bar{q}}]$

sults in four potentials $V^{\alpha\beta}$ respectively coupling $\nu^\alpha = r\phi^\alpha$ to ν^β . The Pauli $\vec{\sigma}$ matrices in the spinors of Eq. (3) produce the spin-dependent [32] potentials of Table II.

Notice that both the pseudoscalar and scalar equations have a system with two equations. This is the minimal number of relativistic equal time equations. However the spin-dependent interactions couple an extra pair of equations both in the vector and axialvector channels. While the coupling of the s -wave and the d -wave are standard in

vectors, the coupling of the spin-singlet and spin-triplet in axialvectors only occurs if the quark and antiquark masses are different, say in heavy-light systems. I now combine the algebraic matrix elements of Table I with the spin-dependent potentials of Table II, to derive the full Salpeter-RPA radial boundstate equations (where the infrared U is dropped from now on). I get the $J^P = 0^-, {}^1S_0$ pseudoscalar (P) equations,

$$\left\{ \left(-\frac{d^2}{dk^2} + E_q(k) + E_{\bar{q}}(k) + \frac{\varphi_q'^2 + \varphi_{\bar{q}}'^2}{4} + \frac{1 - S_q S_{\bar{q}}}{k^2} \right) \begin{bmatrix} 1 & 0 \\ 0 & 1 \end{bmatrix} + \left(\frac{\varphi_q' \varphi_{\bar{q}}'}{2} + \frac{C_q C_{\bar{q}}}{k^2} \right) \begin{bmatrix} 0 & 1 \\ 1 & 0 \end{bmatrix} - M \begin{bmatrix} 1 & 0 \\ 0 & -1 \end{bmatrix} \right\} \begin{pmatrix} \nu_{1S_0}^+(k) \\ \nu_{1S_0}^-(k) \end{pmatrix} = 0, \quad (7)$$

the $J^P = 0^+, {}^3P_0$ scalar (S) equations,

$$\left\{ \left(-\frac{d^2}{dk^2} + E_q(k) + E_{\bar{q}}(k) + \frac{\varphi_q'^2 + \varphi_{\bar{q}}'^2}{4} + \frac{1 + S_q S_{\bar{q}}}{k^2} \right) \begin{bmatrix} 1 & 0 \\ 0 & 1 \end{bmatrix} + \left(\frac{\varphi_q' \varphi_{\bar{q}}'}{2} - \frac{C_q C_{\bar{q}}}{k^2} \right) \begin{bmatrix} 0 & 1 \\ 1 & 0 \end{bmatrix} - M \begin{bmatrix} 1 & 0 \\ 0 & -1 \end{bmatrix} \right\} \begin{pmatrix} \nu_{3P_0}^+(k) \\ \nu_{3P_0}^-(k) \end{pmatrix} = 0. \quad (8)$$

the $J^P = 1^-,$ coupled 3S_1 and 3D_1 vector (V and V^*) equations,

$$\begin{aligned} & \left\{ \left(-\frac{d^2}{dk^2} + E_q(k) + E_{\bar{q}}(k) + \frac{\varphi_q'^2 + \varphi_{\bar{q}}'^2}{4} + \frac{7 - 4S_q - 4S_{\bar{q}} + S_q S_{\bar{q}}}{3k^2} \right) \begin{bmatrix} 1 & 0 & 0 & 0 \\ 0 & 1 & 0 & 0 \\ 0 & 0 & 0 & 0 \\ 0 & 0 & 0 & 0 \end{bmatrix} \right. \\ & + \left(-\frac{\varphi_q' \varphi_{\bar{q}}'}{6} - \frac{C_q C_{\bar{q}}}{3k^2} \right) \begin{bmatrix} 0 & 1 & 0 & 0 \\ 1 & 0 & 0 & 0 \\ 0 & 0 & 0 & 0 \\ 0 & 0 & 0 & 0 \end{bmatrix} + \left(-\frac{d^2}{dk^2} + E_q(k) + E_{\bar{q}}(k) + \frac{\varphi_q'^2 + \varphi_{\bar{q}}'^2}{4} + \frac{8 + 4S_q + 4S_{\bar{q}} + 2S_q S_{\bar{q}}}{3k^2} \right) \\ & \times \begin{bmatrix} 0 & 0 & 0 & 0 \\ 0 & 0 & 0 & 0 \\ 0 & 0 & 1 & 0 \\ 0 & 0 & 0 & 1 \end{bmatrix} + \left(\frac{\varphi_q' \varphi_{\bar{q}}'}{6} - \frac{2C_q C_{\bar{q}}}{3k^2} \right) \begin{bmatrix} 0 & 0 & 0 & 0 \\ 0 & 0 & 0 & 1 \\ 0 & 0 & 1 & 0 \\ 0 & 0 & 1 & 0 \end{bmatrix} - \frac{(1 - S_q)(1 - S_{\bar{q}})}{3k^2} \begin{bmatrix} 0 & 0 & \sqrt{2} & 0 \\ 0 & 0 & 0 & \sqrt{2} \\ \sqrt{2} & 0 & 0 & 0 \\ 0 & \sqrt{2} & 0 & 0 \end{bmatrix} \\ & \left. - \left(\frac{\varphi_q' \varphi_{\bar{q}}'}{3} - \frac{C_q C_{\bar{q}}}{3k^2} \right) \begin{bmatrix} 0 & 0 & 0 & \sqrt{2} \\ 0 & 0 & \sqrt{2} & 0 \\ 0 & \sqrt{2} & 0 & 0 \\ \sqrt{2} & 0 & 0 & 0 \end{bmatrix} - M \begin{bmatrix} 1 & 0 & 0 & 0 \\ 0 & -1 & 0 & 0 \\ 0 & 0 & 1 & 0 \\ 0 & 0 & 0 & -1 \end{bmatrix} \right\} \begin{pmatrix} \nu_{3S_1}^+(k) \\ \nu_{3S_1}^-(k) \\ \nu_{3D_1}^+(k) \\ \nu_{3D_1}^-(k) \end{pmatrix} = 0, \quad (9) \end{aligned}$$

the $J^P = 1^+,$ coupled 1P_1 and 3P_1 axialvector (A and A^*) equations

$$\begin{aligned}
& \left\{ \left(-\frac{d^2}{dk^2} + E_q(k) + E_{\bar{q}}(k) + \frac{\varphi_q'^2 + \varphi_{\bar{q}}'^2}{4} + \frac{3 - S_q S_{\bar{q}}}{k^2} \right) \begin{bmatrix} 1 & 0 & 0 & 0 \\ 0 & 1 & 0 & 0 \\ 0 & 0 & 0 & 0 \\ 0 & 0 & 0 & 0 \end{bmatrix} + \left(\frac{\varphi_q' \varphi_{\bar{q}}'}{2} + \frac{C_q C_{\bar{q}}}{k^2} \right) \begin{bmatrix} 0 & 1 & 0 & 0 \\ 1 & 0 & 0 & 0 \\ 0 & 0 & 0 & 0 \\ 0 & 0 & 0 & 0 \end{bmatrix} \right. \\
& \times \left(-\frac{d^2}{dk^2} + E_q(k) + E_{\bar{q}}(k) + \frac{\varphi_q'^2 + \varphi_{\bar{q}}'^2}{4} + \frac{2}{k^2} \right) \begin{bmatrix} 0 & 0 & 0 & 0 \\ 0 & 0 & 0 & 0 \\ 0 & 0 & 1 & 0 \\ 0 & 0 & 0 & 1 \end{bmatrix} + \left(-\frac{\varphi_q' \varphi_{\bar{q}}'}{2} \right) \begin{bmatrix} 0 & 0 & 0 & 0 \\ 0 & 0 & 0 & 0 \\ 0 & 0 & 0 & 1 \\ 0 & 0 & 1 & 0 \end{bmatrix} \\
& \left. + \frac{S_q - S_{\bar{q}}}{k^2} \begin{bmatrix} 0 & 0 & \sqrt{2} & 0 \\ 0 & 0 & 0 & \sqrt{2} \\ \sqrt{2} & 0 & 0 & 0 \\ 0 & \sqrt{2} & 0 & 0 \end{bmatrix} - M \begin{bmatrix} 1 & 0 & 0 & 0 \\ 0 & -1 & 0 & 0 \\ 0 & 0 & 1 & 0 \\ 0 & 0 & 0 & -1 \end{bmatrix} \right\} \begin{pmatrix} \nu_{1P_1}^+(k) \\ \nu_{1P_1}^-(k) \\ \nu_{3P_1}^+(k) \\ \nu_{3P_1}^-(k) \end{pmatrix} = 0, \quad (10)
\end{aligned}$$

III. NUMERICAL SOLUTION OF THE MASS GAP AND BOUNDSTATE EQUATIONS AT $T = 0$

Notice that this model, like any chiral model, has the same number of meson states in the spectrum as the normal quark model. The mass splittings can be related, as usual, to spin-tensor potentials. It is interesting to study chiral symmetry when the quark and antiquark are light, and to study the chiral and heavy-quark symmetry when, say, the quark is light and the antiquark is heavy.

In the light-light case, the chiral invariant vacuum is reached in the limit of $m_q = m_{\bar{q}} \rightarrow 0$. The chiral angle, the sine and the cosine of the chiral angle have limits $\varphi \rightarrow 0$, $S \rightarrow 0$, $C \rightarrow 1$. Then, if we transform Eq. (8) with the transformation matrix,

$$\begin{pmatrix} \nu_{3P_0}^+(k) \\ \nu_{3P_0}^-(k) \end{pmatrix} \rightarrow \begin{bmatrix} 1 & 0 \\ 0 & -1 \end{bmatrix} \begin{pmatrix} \nu_{3P_0}^+(k) \\ \nu_{3P_0}^-(k) \end{pmatrix}, \quad (11)$$

it is clear that both Eq. (7) and (8) become identical to,

$$\begin{cases} \left(-\frac{d^2}{dk^2} + 2k - \frac{1}{k^2} - M \right) \nu^+(k) + \frac{1}{k^2} \nu^-(k) = 0 \\ \frac{1}{k^2} \nu^+(k) + \left(-\frac{d^2}{dk^2} + 2k - \frac{1}{k^2} + M \right) \nu^-(k) = 0 \end{cases}. \quad (12)$$

The vector and axialvector equations have the double of solutions of the pseudoscalar and scalar. To separate them, they are from now on, respectively, called V, V^* and A, A^* . In the same light-light limit, Eq. (9) can be block diagonalized [17] with the transformation,

$$\begin{pmatrix} \nu_{3S_1}^+(k) \\ \nu_{3S_1}^-(k) \\ \nu_{3D_1}^+(k) \\ \nu_{3D_1}^-(k) \end{pmatrix} \rightarrow \begin{bmatrix} -\frac{1}{\sqrt{3}} & 0 & \frac{\sqrt{2}}{3} & 0 \\ 0 & -\frac{1}{\sqrt{3}} & 0 & \frac{\sqrt{2}}{3} \\ \frac{\sqrt{2}}{3} & 0 & \frac{1}{\sqrt{3}} & 0 \\ 0 & \frac{\sqrt{2}}{3} & 0 & \frac{1}{\sqrt{3}} \end{bmatrix} \begin{pmatrix} \nu_{3S_1}^+(k) \\ \nu_{3S_1}^-(k) \\ \nu_{3D_1}^+(k) \\ \nu_{3D_1}^-(k) \end{pmatrix} \quad (13)$$

and each block V and V^* , with mixed s -wave and d -wave, is identical one of the two independent blocks of Eq. (10),

$$\begin{cases} \left(-\frac{d^2}{dk^2} + 2k + \frac{1}{k^2} - M \right) \nu^+(k) + \frac{1}{k^2} \nu^-(k) = 0 \\ \frac{1}{k^2} \nu^+(k) + \left(-\frac{d^2}{dk^2} + 2k + \frac{1}{k^2} + M \right) \nu^-(k) = 0 \end{cases}, \quad (14)$$

$$\begin{cases} \left(-\frac{d^2}{dk^2} + 2k - M \right) \nu^+(k) = 0 \\ \left(-\frac{d^2}{dk^2} + 2k + M \right) \nu^-(k) = 0 \end{cases}.$$

This checks that the chiral partners P - S and V, V^* - A, A^* are degenerate in the false chiral symmetric vacuum.

Another interesting case is the heavy-light case [27] where, say, the antiquark has a mass $m_{\bar{q}} \simeq m_{0\bar{q}} \gg K_0$. Then the negative energy components ν^- vanish, like in nonrelativistic quark models, and there are no Tachyons. In the infinite $m_{\bar{q}}$ case, $S_{\bar{q}} = 1$, $C_{\bar{q}} = 0$, $G_{\bar{q}} = 0$, and the antiquark spin becomes irrelevant, see Table II, complying with the Isgur-Wise heavy-quark symmetry.

In this case the degeneracy is even larger than in the light-light case. Because the heavy-quark spin does not contribute to the spectrum, the 1S_0 pseudoscalar P and the 3S_1 vector V are degenerate, for any light quark mass m_q . Now in the limit of a vanishing light quark mass $m_q \rightarrow 0$, chiral symmetry implies that the scalar S is degenerate with the pseudoscalar P and that the axialvector A is degenerate with the vector V . Thus in the chiral invariant vacuum all four mesons P, V, S, A are degenerate.

In what concerns the second vector V^* and the second axial A^* , they are degenerate with tensor mesons. Notice also that the heavy antiquark mass kills the tensor potential, and thus the d -wave component of the vector decouples from the s -wave. The V^* is a pure d -wave vector. Differently from the light-light case, now the axialvector A equation is not diagonal. In the limit of the massless quark, the axialvector equation can be diagonalized with the transformation,

$$\begin{pmatrix} \nu_{1P_1}^+(k) \\ \nu_{3P_1}^+(k) \end{pmatrix} \rightarrow \begin{bmatrix} -\sqrt{\frac{2}{3}} & \frac{1}{\sqrt{3}} \\ \frac{1}{\sqrt{3}} & -\sqrt{\frac{2}{3}} \end{bmatrix} \begin{pmatrix} \nu_{1P_1}^+(k) \\ \nu_{3P_1}^+(k) \end{pmatrix}, \quad (15)$$

and the two diagonalized axialvector equations are identical to the vector V and V^* equations.

For the numerical solution, I change the sign of the second and fourth lines in Eqs. (7) to (10) and then I get a simple eigenvalue equation. I solve the equation diagonalizing the Salpeter-RPA matrix replacing the second derivative with finite differences. Other numerical methods can also be used [19]. The results are shown in Figs. 2–5.

In Fig. 2, the pseudoscalar P and scalar S light quark and light antiquark meson masses are interpolated from the true spontaneously chiral symmetry breaking vacuum to the false chiral restored vacuum. In Fig. 3, the vector V , V^* and axial A , A^* light quark and light antiquark meson masses are interpolated from the true spontaneously chiral symmetry breaking vacuum to the false chiral restored

vacuum. In Fig. 4, the pseudoscalar P and vector V , and the scalar S and axialvector A , light quark and heavy antiquark meson masses are interpolated from the true spontaneously chiral symmetry breaking vacuum to the false chiral restored vacuum. In Fig. 5, the vector V^* and axialvector A^* light quark and heavy antiquark meson masses are interpolated from the true spontaneously chiral symmetry breaking vacuum to the false chiral restored vacuum. Notice that in the false chiral restored vacuum, all Figs. 2–5 are compatible with the chiral degeneracies predicted in Eqs. (12) and (14).

A remarkable result of the numerical finite difference solutions is that all studied light-light pseudoscalar and scalar mesons, including all radial excitations, become tachyons, with arbitrarily large imaginary masses. This will be confirmed in the next Sec. IV.

On the other hand, all the other mesons suffer small mass over potential strength M/K_0 corrections from one vacuum to the other. Notice however that the potential

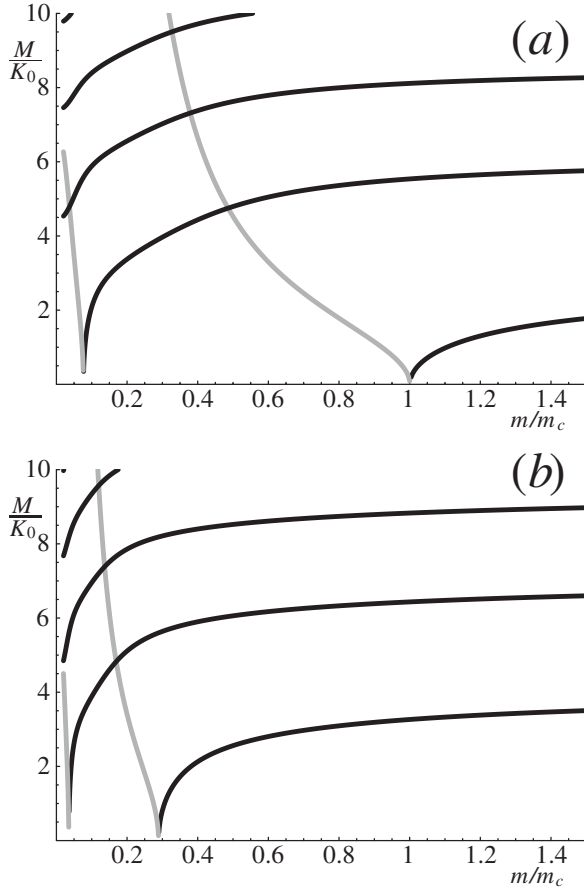


FIG. 2. Light-light meson masses, in (a), pseudoscalar P , in (b), scalar S , when the light quark mass interpolates from the zero mass of the chiral invariant false vacuum to the solution m_c of the mass gap equation in the true vacuum. The dark curves correspond to mesonic real masses and the light curves correspond to tachyonic imaginary masses.

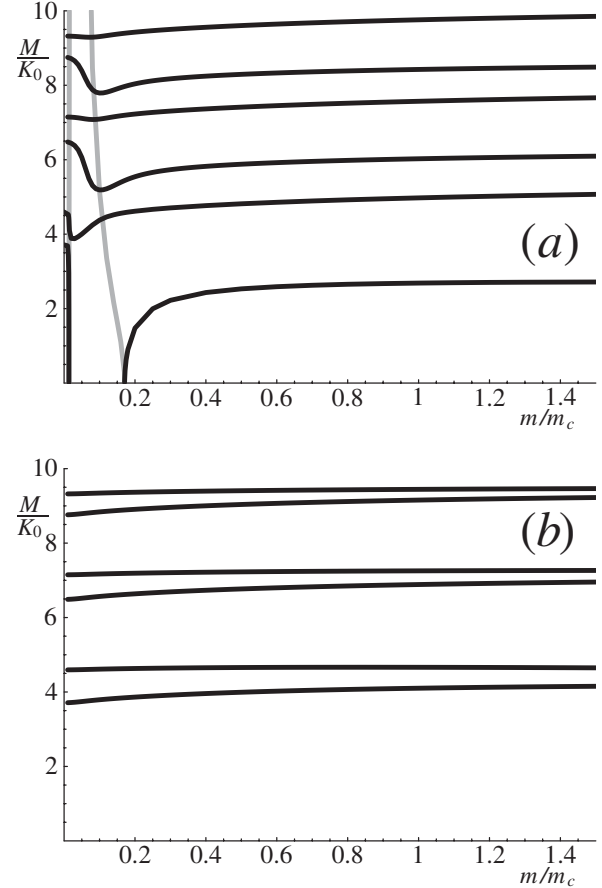


FIG. 3. Light-light meson masses, in (a), vector V , V^* and in (b), axialvector A , A^* , when the light quark mass interpolates from the zero mass of the chiral invariant false vacuum to the solution m_c of the mass gap equation in the true vacuum. The dark curves correspond to mesonic real masses and the light curves correspond to tachyonic masses.

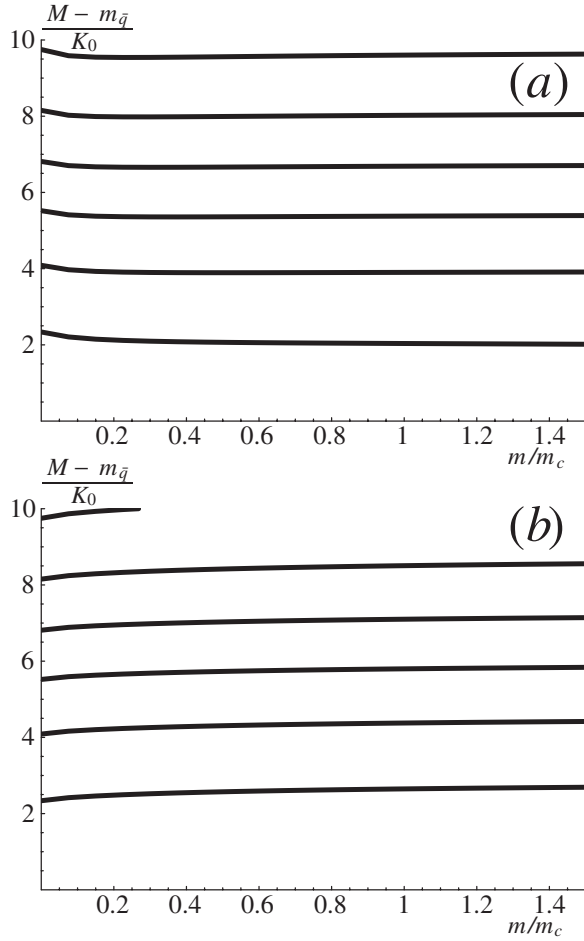


FIG. 4. Heavy-light meson masses minus the infinitely heavy antiquark mass, in (a), pseudoscalar and first vector, in (b), scalar and first axialvector, when the light quark mass interpolates from the zero mass of the chiral invariant false vacuum to the solution m_c of the mass gap equation in the true vacuum. In this case there are no tachyonic imaginary masses.

strength K_0 is expected to change significantly when the vacuum is changed. This will be discussed in detail in Sec. V.

A remarkable feature of the light-light vector meson groundstate in Fig. 2 may be relevant for the ρ and ω mesons. Although the M/K_0 corrections from one vacuum to the other are small, at small but nonvanishing quark mass the groundstate vector meson is a tachyon. This occurs just before the vector and axial vector are degenerate. Because the actual light current quark masses are small but nonvanishing, this will be addressed in Sec. V.

IV. ANALYTICAL STUDY OF THE TACHYONS

I now study in detail the properties of the eigenvalues of the Salpeter or RPA equations. Here only the light-light systems is studied in detail, because tachyons do not occur in the heavy-light systems.

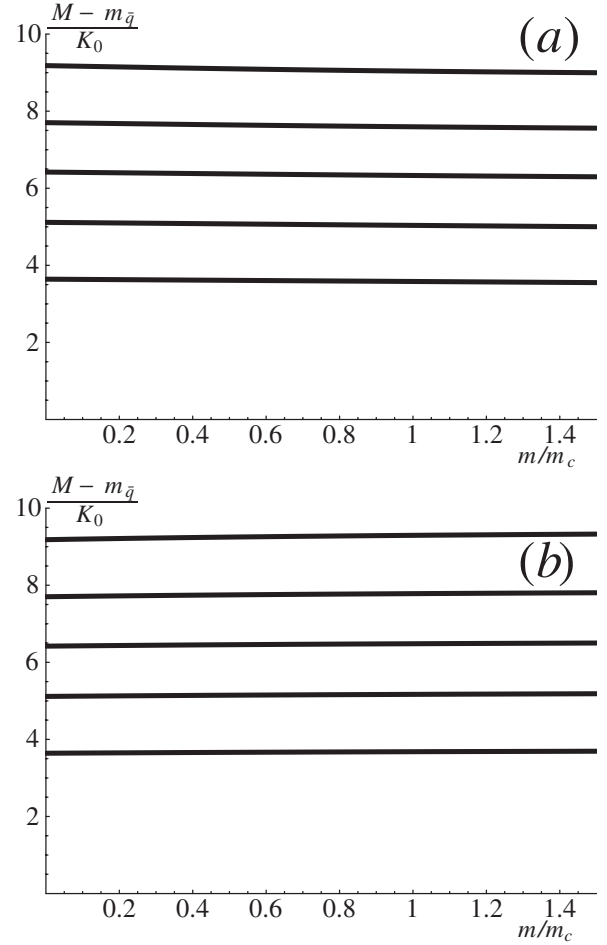


FIG. 5. Heavy-light meson masses minus the infinitely heavy antiquark mass, in (a), second vector V^* and in (b), second axialvector A^* , when the light quark mass interpolates from the zero mass of the chiral invariant false vacuum to the solution m_c of the mass gap equation in the true vacuum. In this case there are no tachyonic imaginary masses.

The boundstate equation can be decoupled,

$$\begin{aligned}
 & \begin{cases} H\nu^+ + V\nu^- = M\nu^+ \\ H\nu^+ + V\nu^- = -M\nu^- \end{cases} \\
 & \Rightarrow \begin{cases} (H + V)(\nu^+ + \nu^-) = M(\nu^+ - \nu^-) \\ (H - V)(\nu^+ - \nu^-) = M(\nu^+ + \nu^-) \end{cases} \\
 & \Rightarrow \begin{cases} (H - V)(H + V)(\nu^+ + \nu^-) = M^2(\nu^+ + \nu^-) \\ (H + V)(H - V)(\nu^+ - \nu^-) = M^2(\nu^+ - \nu^-) \end{cases} .
 \end{aligned} \tag{16}$$

Thus we get a pair of eigenvalue equations, where H and V are hermitean, but $(H - V)(H + V)$ and $(H + V)(H - V)$ are not hermitean. Nevertheless M^2 can be proved to be real, if one considers two different eigenvalues M_1^2 and M_2^2 ,

$$\begin{cases} (H - V)(H + V)(\nu_1^+ + \nu_1^-) = M_1^2(\nu_1^+ + \nu_1^-) \\ (\nu_2^+ - \nu_2^-)^\dagger(H - V)(H + V) = (\nu_2^+ - \nu_2^-)^\dagger M_2^{2*} \\ \Rightarrow \begin{cases} (M_1^2 - M_2^{2*})(\nu_2^+ - \nu_2^-)^\dagger(\nu_1^+ + \nu_1^-) = 0 \\ (M_2^2 - M_1^{2*})(\nu_1^+ - \nu_1^-)^\dagger(\nu_2^+ + \nu_2^-) = 0 \end{cases} \end{cases} \quad (17)$$

Notice that the orthonormalization condition [17,19,20] of the Salpeter-RPA equation is,

$$(\nu_i^{+\dagger}, \nu_i^{-\dagger}) \begin{bmatrix} 1 & 0 \\ 0 & -1 \end{bmatrix} \begin{pmatrix} \nu_j^+ \\ \nu_j^- \end{pmatrix} = \delta_{i,j}. \quad (18)$$

Thus, either the two eigenvectors are orthogonal or the squared eigenvalue M^2 is real. This shows that the solutions of the boundstate equation can only have real or purely imaginary masses. While the real masses correspond to mesons, the imaginary masses correspond to tachyons.

I now study in detail the solutions in the chiral invariant vacuum and in the chiral limit, where both the current mass m_0 and the constituent mass m_c vanish. In general the boundstate equations decouple in two different equations, one for $J \geq 0$ with,

$$\begin{cases} H = -\frac{d^2}{dk^2} + 2k - \frac{1}{k^2} + \frac{j(j+1)}{k^2} \\ V = \frac{1}{k^2} \end{cases}, \quad (19)$$

and another for $J \geq 1$ with,

$$\begin{cases} H = -\frac{d^2}{dk^2} + 2k - \frac{2}{k^2} + \frac{j(j+1)}{k^2} \\ V = \frac{0}{k^2} \end{cases}. \quad (20)$$

The Eqs. (12) and (14) constitute particular cases of Eqs. (19) and (20). Notice that the different potentials $-\frac{d^2}{dk^2}$, $2k$, $\frac{1}{k^2}$ are bound from below and positive definite in the sense that all their eigenvalues are positive. However $-\frac{1}{k^2}$ is unbound from below. Thus, in Eq. (17) all terms $H + V$ or $H - V$ are positive definite and bound from below, except for the $H - V$ of the $J = 0$ pseudoscalar and scalar tachyons in Eq. (19).

Notice that Fig. 2 suggests that all pseudoscalars and scalars become tachyons in the chiral invariant vacuum. To confirm this suggestion of an infinite number of tachyons it is convenient to regularize the scalar and pseudoscalar equations, because the wave-functions are concentrated at extremely small distances. A very small quark mass m is assumed constant for simplicity, and the momentum and mass are rescaled,

$$k/m \rightarrow k', \quad Mm^2 \rightarrow M'. \quad (21)$$

Notice that any finite solution M' in fact corresponds to an infinite mass $M = M'/m^2$, and that a wave-function with a finite k' corresponds to a wave-function with infinitesimal momentum $k = k'm$. Then, starting from Eq. (7) one gets for the pseudoscalar,

$$\begin{cases} H + V = -\frac{d^2}{dk'^2} \\ H - V = -\frac{d^2}{dk'^2} - \frac{2}{k'^2+1} - \frac{1}{(k'^2+1)^2} \end{cases}, \quad (22)$$

respectively positive definite and with negative eigenvalues, and from Eq. (8) one gets for the scalar,

$$\begin{cases} H - V = -\frac{d^2}{dk'^2} + \frac{2}{k'^2(k'^2+1)} - \frac{1}{(k'^2+1)^2} \\ H + V = -\frac{d^2}{dk'^2} + \frac{2}{k'^2(k'^2+1)} - \frac{2}{k'^2+1} \end{cases}, \quad (23)$$

respectively positive definite and with negative eigenvalues. An irrelevant term $m^3 2k'/\sqrt{k'^2+1}$ is also present in the rescaled equations.

The Bohr-Sommerfeld quantization condition can be used to count the number of negative eigenvalues of the $H - V$ pseudoscalar operator and of the $H + V$ scalar operator. The leading term at high momentum, assuming the highest possible negative mass $M' \simeq 0$, is,

$$\int_0^\infty \sqrt{\frac{1}{1+k'^2}} dk' = \infty. \quad (24)$$

This shows that the number of tachyons in the pseudoscalar and scalar channels are both infinite.

This is confirmed by the numerical solution of the regularized Salpeter equation. In Table III we show the masses of the different light-light tachyons and mesons in the chiral invariant false vacuum and in the chiral limit. Le Yaouanc *et al.* [17] have already shown that the pseudoscalar Eq. (7) and the scalar Eq. (8) possess takyonic solutions. Here we find that the number of tachyons is infinite, and that they all have infinite masses in the chiral invariant false vacuum and in the chiral limit

Notice that, because the rescaled equations depend on a quark mass m , very small but finite, there is no pseudoscalar-scalar degeneracy in the rescaled equations. Since the equations are different, $M'_S \neq M'_P$. Nevertheless in the limit $m \rightarrow 0$ of the chiral invariant vacuum, both

TABLE III. Masses of the first angular and radial excitations of the different light-light tachyons and mesons in the chiral invariant false vacuum and in the chiral limit. Each column includes both positive and negative parity degenerate states, except for the pseudoscalar and scalar tachyonic states. Notice that the tachyon masses are infinite and that they are regularized by an arbitrarily small quark mass m . The meson masses are separated in two different families with the same J because two different equations decouple for each J .

n	Pse	Sca	$J = 1$	$J = 1$	$J = 2$	$J = 2$	$J = 3$	$J = 3$
0	$\frac{2 \times 10^{-1} i}{m^2}$	$\frac{3 \times 10^{-2} i}{m^2}$	3.71	4.59	6.15	6.45	7.65	7.84
1	$\frac{2 \times 10^{-3} i}{m^2}$	$\frac{3 \times 10^{-4} i}{m^2}$	6.49	7.15	8.43	8.69	9.72	9.89
2	$\frac{2 \times 10^{-5} i}{m^2}$	$\frac{3 \times 10^{-6} i}{m^2}$	8.76	9.32	10.45	10.68	11.61	11.76
3	$\frac{2 \times 10^{-7} i}{m^2}$	$\frac{3 \times 10^{-8} i}{m^2}$	10.77	11.27	12.30	12.51	13.38	13.52
4	$\frac{2 \times 10^{-9} i}{m^2}$	$\frac{3 \times 10^{-10} i}{m^2}$	12.61	13.08	14.05	14.25	15.12	15.26

pseudoscalar and scalar tachyons have infinite imaginary masses. Because the infinities are identical, in the $m \rightarrow 0$ limit one gets $M_S = M_P = \infty i$. Tachyons comply with the chiral degeneracy in a subtle way.

V. CONCLUSION, INCLUDING TEMPERATURE EFFECTS

Assuming a confining potential, the mass M spectrum of mesons is studied in the true chiral symmetry breaking vacuum and in the unstable vacuum where chiral symmetry restoration occurs. The only parameter is the strength K_0 of the potential. Chiral models have the same number of meson states in the spectrum as the normal quark model. The mass splittings can be related, as usual, to spin-tensor potentials. In the limit of vanishing constituent quark masses, all spin-dependent potentials are quite simple, proportional to K_0^3/k^2 .

In the chiral limit the mesons suffer small M/K_0 changes from one vacuum to the other, except for the $J = 0$ pseudoscalars and scalars. All the $J = 0$ mesons, including all possible radial excitations, are transformed in tachyons with infinite imaginary masses, when the true vacuum is replaced by the chiral invariant vacuum. A detailed analytical proof and a precise numerical study of the tachyons are also presented here.

However, before moving to the conclusions, these beautiful mathematical results should be matched with our knowledge of the deconfined phase of QCD.

My first comment concerns the calibration problem of any chiral symmetric model. The Sigma Model, the Nambu and Jona-Lasinio model and Chiral Lagrangian estimations are not confining and thus are not expected to address correctly hadrons with spin, angular or radial excitations. The present model is adequate to study the angular or radial excitations of hadrons, and in this sense it already upgrades previous estimations of the meson spectra in the chiral restored vacuum. Nevertheless the present density-density interaction suffers from uncalibrated spin-tensor potentials. But I assume that the under development chiral invariant quark models with a confining funnel interaction [21,33] a vector interaction [20,34], or long range scalar interactions [35,36], can be correctly calibrated. Nevertheless, for a qualitative study, the present density-density harmonic confining interaction should be sufficient, since PB and Nefediev [18] have shown that this interaction has similar mass gap solutions to the other possible confining potentials in Coulomb gauge QCD.

My second comment concerns the parameters of the present model. The potential strength K_0 , the dominant scale of the present study, is expected to change from the ordinary QCD vacuum to the deconfined phase of QCD. This is quite important because the meson masses scale with K_0 .

My first conclusion concerns corrections due to the current quark mass. The light current quark mass is small

but not vanishing. The u or d quarks correspond to and increase the chiral limit quark constituent mass by 1% to 2% of m_c , while the s quark amounts to increase the chiral limit quark constituent mass by up to 50%. For instance in the true vacuum the s constituent quark mass is of the order of $1.5m_c$, while in the chiral restored vacuum the s constituent quark mass is of the order of $0.5m_c$. These simple factors are sufficient to estimate from the Figs. 2–5, the masses of the vectors ρ , ω or ϕ , or of the pseudoscalar and vector D and D_s , relevant for the new di-muon measurements of NA60. In the light-light systems, with a u or d quark and a \bar{u} or \bar{d} antiquark, the number and the imaginary mass of pseudoscalar and scalar tachyons are not infinite, nevertheless they are very large. Also, with a finite current quark mass, the pseudoscalar instability may be larger (more tachyons, with larger imaginary mass) than the scalar instability.

Interestingly, in Fig. 3 the vector meson has real mass for zero quark masses, but for a small mass the vector meson is a tachyon. Thus it is possible that the ρ meson, or the ω meson, simply disappear in the chiral restored vacuum. Because the quark mass interval, where the vector meson is a tachyon, is quite small, it is plausible that the ρ meson and the ω meson may have a different tachyonic behavior, although the present study cannot explore the differences between the ρ and the ω . Notice that the NA60 collaboration saw differences between the production rate of the ρ and the ω [1–5], but this may also be due to ρ interactions with π at the periphery of the deconfined QCD bubble [37].

My second conclusion is that the chiral invariant vacuum is too unstable to be reached, unless confinement is lost. This is clearly signalled by the infinite, (or very large) number of infinite (or very large) imaginary mass of tachyons in the pseudoscalar and scalar channels. This extreme instability confirms a result of Le Yaouanc *et al.* [16], who studied the deconfinement transition, using the present confining potential, and concluded that the transition does not occur for any finite temperature. Therefore a change in the potential must happen before the chiral restoration transition occurs. This also confirms the lattice QCD simulations initiated by Kogut, Wyld, Karsch and Sinclair [38–40], and the Schwinger-Dyson calculations initiated by Bender, Blaschke, Kalinovsky and Roberts, [41,42] who also found a restoration of chiral symmetry coincident with the loss of confinement at temperatures of the order of 150 MeV.

The third conclusion of this paper is that all the meson masses are much smaller in the high temperature chiral invariant vacuum, than they are in the low temperature symmetry breaking vacuum. Notice for instance that the apparently constant vector and axialvector masses of Fig. 5 are proportional to the potential strength K_0 , thus they decrease when the potential strength decreases. This is an educated conclusion, based on Lattice QCD simulations of

the dependence of the confining potential with temperature and also with dynamical fermions. when confinement is lost, [40] at temperatures of the order of 150 MeV, the strength of the potential is also decreased. These two effects are necessary for chiral symmetry restoration.

Assuming these two changes, both in shape and strength of the potential, the spectra computed in this paper can be reinterpreted. Assuming that confinement disappears, the infinite number of infinite imaginary mass tachyons go away. Moreover, a smaller strength of the potential is also necessary to remove any tachyon in the chiral symmetric vacuum. Then the chiral symmetric vacuum is the only and true vacuum. Notice that, for light quarks, the largely dominant scale, including the scale ruling the constituent quark mass, is the strength of the potential. All the spectra are proportional to the strength of the potential, see

Figs. 2–5. Then, with a much weaker potential, the masses and widths of any possible mesons are much smaller (except for the contribution of the heavy-quark mass, say the \bar{c} mass in D or D_s mesons) than the masses of ordinary mesons listed by the Particle Data Group [43]. Thus the vector mesons identified by the NA60 collaboration, with masses close to the ordinary masses, are not expected to be probed inside the deconfined phase of QCD, where all mesons, if any, are much lighter.

ACKNOWLEDGMENTS

P. B. thanks João Seixas for extremely motivating discussions on the results of NA60 and on lattice QCD potentials.

-
- [1] R. Arnaldi *et al.* (NA60 Collaboration), Phys. Rev. Lett. **96**, 162302 (2006).
 - [2] S. Damjanovic *et al.* (NA60 Collaboration), J. Phys. G **31**, S903 (2005).
 - [3] S. Damjanovic *et al.* (NA60 Collaboration), nucl-ex/0510044.
 - [4] H. K. Woehri *et al.* (NA60 Collaboration), Eur. Phys. J. C **43**, 407 (2005).
 - [5] H. K. Woehri *et al.* (NA60 Collaboration), Proc. Sci., HEP2005 (2006) 132.
 - [6] G. E. Brown and M. Rho, Phys. Rev. Lett. **66**, 2720 (1991).
 - [7] G. E. Brown and M. Rho, Phys. Rep. **269**, 333 (1996).
 - [8] G. E. Brown and M. Rho, Phys. Rep. **363**, 85 (2002).
 - [9] G. E. Brown and M. Rho, Phys. Rep. **398**, 301 (2004).
 - [10] J. S. Schwinger, Ann. Phys. (N.Y.) **2**, 407 (1957).
 - [11] M. Gell-Mann and M. Levy, Nuovo Cimento **16**, 705 (1960).
 - [12] M. D. Scadron, F. Kleefeld, and G. Rupp, hep-ph/0601196.
 - [13] Y. Nambu and G. Jona-Lasinio, Phys. Rev. **122**, 345 (1961); **124**, 246 (1961).
 - [14] A. A. Osipov, B. Hiller, V. Bernard, and A. H. Blin, hep-ph/0507226; A. A. Osipov, B. Hiller, and J. da Providencia, Phys. Lett. B **634**, 48 (2006); A. A. Osipov, B. Hiller, J. Moreira, and A. H. Blin, Eur. Phys. J. C **46**, 225 (2006); B. Hiller, A. A. Osipov, V. Bernard, and A. H. Blin, SIGMAP bulletin **2**, 026 (2006).
 - [15] G. 't Hooft, Phys. Rev. D **14**, 3432 (1976); **18**, 2199(E) (1978).
 - [16] A. Le Yaouanc, L. Oliver, O. Pène, J. C. Raynal, M. Jarfi, and O. Lazrak, Phys. Rev. D **38**, 3256 (1988); **37**, 3702 (1988); **37**, 3691 (1988).
 - [17] A. Le Yaouanc, L. Oliver, S. Ono, O. Pène, and J. C. Raynal, Phys. Rev. D **31**, 137 (1985).
 - [18] P. J. A. Bicudo and A. V. Nefediev, Phys. Rev. D **68**, 065021 (2003).
 - [19] P. Bicudo and J. E. Ribeiro, Phys. Rev. D **42**, 1611 (1990); **42**, 1625 (1990); **42**, 1635 (1990).
 - [20] P. Bicudo, Phys. Rev. C **60**, 035209 (1999).
 - [21] F. J. Llanes-Estrada and S. R. Cotanch, Phys. Rev. Lett. **84**, 1102 (2000).
 - [22] P. Bicudo, Phys. Rev. C **67**, 035201 (2003).
 - [23] P. Bicudo, S. Cotanch, F. Llanes-Estrada, P. Maris, J. E. Ribeiro, and A. Szczepaniak, Phys. Rev. D **65**, 076008 (2002).
 - [24] P. Bicudo, M. Faria, G. M. Marques, and J. E. Ribeiro, Nucl. Phys. A **735**, 138 (2004).
 - [25] R. Delbourgo and M. D. Scadron, J. Phys. G **5**, 1621 (1979).
 - [26] F. J. Llanes-Estrada and P. Bicudo, Phys. Rev. D **68**, 094014 (2003).
 - [27] P. Bicudo, hep-ph/0512041.
 - [28] P. Bicudo, N. Brambilla, E. Ribeiro, and A. Vairo, Phys. Lett. B **442**, 349 (1998).
 - [29] H. G. Dosch and Y. A. Simonov, Phys. Lett. B **205**, 339 (1988).
 - [30] Y. S. Kalashnikova, A. V. Nefediev, and J. E. F. Ribeiro, Phys. Rev. D **72**, 034020 (2005).
 - [31] A. V. Nefediev, Pis'ma Zh. Eksp. Teor. Fiz. **78**, 801 (2003) [JETP Lett. **78**, 349 (2003)].
 - [32] P. Bicudo, G. Krein, J. E. F. Ribeiro, and J. E. Villate, Phys. Rev. D **45**, 1673 (1992).
 - [33] P. Bicudo, J. E. Ribeiro, and J. Rodrigues, Phys. Rev. C **52**, 2144 (1995).
 - [34] F. J. Llanes-Estrada and S. R. Cotanch, Nucl. Phys. A **697**, 303 (2002); F. J. Llanes-Estrada, S. R. Cotanch, A. P. Szczepaniak, and E. S. Swanson, Phys. Rev. C **70**, 035202 (2004).
 - [35] P. Bicudo and G. Marques, Phys. Rev. D **70**, 094047 (2004).
 - [36] J. E. Villate, D. S. Liu, J. E. Ribeiro, and P. Bicudo, Phys. Rev. D **47**, 1145 (1993).
 - [37] A. Dobado, A. Gomez Nicola, F. J. Llanes-Estrada, and J. R. Pelaez, Phys. Rev. C **66**, 055201 (2002).
 - [38] J. B. Kogut, H. W. Wyld, F. Karsch, and D. K. Sinclair,

- Phys. Lett. B **188**, 353 (1987).
- [39] R. Narayanan and H. Neuberger, Phys. Lett. B **638**, 546 (2006).
- [40] F. Karsch, Lect. Notes Phys. **583**, 209 (2002).
- [41] A. Bender, D. Blaschke, Y. Kalinovsky, and C. D. Roberts, Phys. Rev. Lett. **77**, 3724 (1996).
- [42] C. D. Roberts and S. M. Schmidt, Prog. Part. Nucl. Phys. **45**, S1 (2000).
- [43] K. Hagiwara *et al.* (Particle Data Group Collaboration), Phys. Rev. D **66**, 010001 (2002).